Pulse Dual Slope Modulation for VLC

Minseok Oh[1]
[1] Department of Electronic Engineering, Kyonggi University
Suwon 443-760, Korea
[e-mail: msoh@kgu.ac.kr]
*Corresponding author: Minseok Oh

Received September 2, 2013; revised November 9, 2013; accepted March 14, 2014; published April 29, 2014

Abstract

In the field of visible light communication (VLC), light-emitting diodes (LEDs) are used for transmitting data via visible light. In this study, we analyze pulse dual slope modulation (PDSM) as a means of delivering information in VLC. PDSM involves the modulation of symmetrical slope pulses to encode binary 0s and 1s, and owing to the moderately increasing and decreasing pulse shapes that are created, this method enables more spectral efficiency than the variable pulse position modulation (VPPM) technique currently adopted in IEEE 802.15.7. In particular, PDSM allows for the avoidance of intra-frame flicker by providing *idle* pulses in a spectrum-efficient way. A simple detection scheme is proposed for PDSM signals, and its bit error rate (BER) is analyzed mathematically at varying slopes to validate the process through simulation. The BER performance of PDSM detection using dual sampling is compared to the performances of PDSM and VPPM using correlation detection. It is found that, when the probability of *idle* pulse transmission is less than 0.08 and higher than 0, the BER of dual sampling PDSM is lower than that of PDSM using correlation detection over the entire light intensity range.

Keywords: Visible light communication, pulse dual slope modulation, PDSM, flicker mitigation, spectral efficiency

http://dx.doi.org/10.3837/tiis.2014.04.007

1. Introduction

As the demand for wireless data transmission increases, the radio frequency spectrum is becoming increasingly congested. Consequently, attention has been drawn toward alternative technologies and frequency bands, and the abundance of unregulated bandwidth at optical frequencies may make optical wireless technologies attractive candidates for use in future local area networks [1]. Optical wireless communications using infrared light-emitting diodes (LEDs) was first proposed by Gfeller and Bapst [2], and optical LED wireless communications in the visible spectral range (380 to 780 nm), which is commonly referred to as visible light communication (VLC), has recently begun to receive increasing attention [3]. IEEE 802.15.7, which produced the first global VLC standard in September 2011, provides standards for dimming-adaptable mechanisms that can be used in flicker-free high-data-rate visible light communication [4-6].

VLC normally involves the transmission of data through modulations of LED light intensity that occur faster than the persistence of the human eye. Although most people cannot perceive flickering at a frequency greater than 100 Hz, the repeated use of a low rate clock may nevertheless generate infrequent flickering. A VLC flicker represents a periodic or non-periodic output power or light intensity fluctuation that can be perceived by human eyes; such flickering can cause eye fatigue or even sight deterioration if exposure is prolonged. To avoid flicker, light intensity changes over periods longer than the maximum flickering time period (MFTP), which is defined as the maximum time period over which a change in light intensity is not perceivable by the human eye [7], must be prevented. In the context of VLC, flicker can be classified alternatively as intra-frame or inter-frame flicker [6]; the former is caused by light intensity discrepancies between the bit patterns representing 1 and 0 within a data frame, whereas the latter is caused by discrepancies in average light intensity between the packet frame transmission and idle periods.

Dimming is an essential functionality of modern LED lighting systems, and variable pulse position modulation (VPPM) seems to provide the most effective means of accurately controlling LED illumination without incurring color rendering in the emitted light [8-11]. In VPPM, light intensity is controlled by adjusting the duty cycle of a pulse train; however, if this is done at low data rates or with long idle periods, the resulting flicker may become more noticeable.

The rest of this article proceeds as follows. Section 2 describes the proposed pulse dual slope modulation (PDSM) scheme and its spectral efficiency. In Section 3, a recovery process at the receiver is proposed, its bit error rate (BER) is calculated as a function of the slope of the rising or falling pulse edge, and the BERs for various settings are analyzed. In addition, the widely used correlation detection method is applied to PDSM and VPPM for comparison purposes. Finally, Section 4 concludes the paper.

2. Pulse Dual Slope Modulation (PDSM)

2.1 Properties of PDSM

PDSM is a modified version of pulse slope modulation (PSM) [12], a method used in analog signaling, and was first proposed by Anand M and P. Mishra [13]. **Fig. 1** shows the three pulse types used in PDSM. A binary input of 0 changes the slope of the rising (or falling) edge of the pulse within the pulse duration while maintaining the slope of the falling (or rising) edge vertical. Similarly, a binary input of 1 changes only the slope of the falling (or rising) edge of the pulse while maintaining the slope of the rising (or falling) edge vertical. By allowing the PDSM to maintain its light source in a constant virtual *on* state, the use of gradually changing pulse shapes can alleviate intra-frame flicker. Here, we will assume that the light intensity of a pulse is proportional to the area it encloses on a time–amplitude graph.

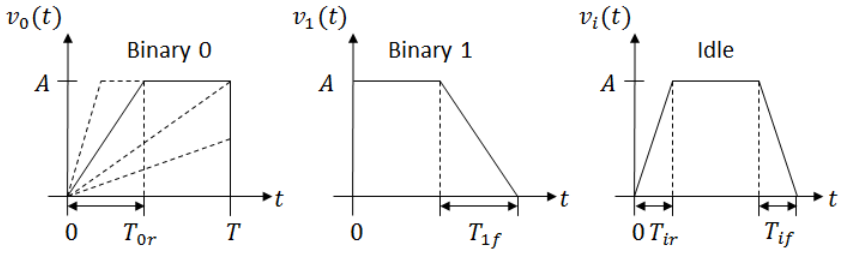

Fig. 1. Pulse dual slope modulation waveform

In this study, the amplitude of a pulse is given by A, and we will assume that a pulse having a moderately rising hypotenuse with a constant absolute magnitude represents binary 0 or 1, depending on the sign of the slope of the hypotenuse. To reduce interframe flicker, we propose using a symmetric pulse to represent an *idle* pattern, as shown in **Fig. 1**. As the average light intensity of the *idle* bit pattern over bit duration T is set equal to that of the data bit, $T_{ir} = T_{if} = \frac{T_{0r}}{2} = \frac{T_{1f}}{2}$, where T_{ir} and T_{if} are the rise and fall times, respectively, of an *idle* pulse, and T_{0r} and T_{1f} are the rise time of a binary 0 pulse and the fall time of a binary 1 pulse, respectively, as shown in the figure. The slope, defined as $s = \frac{A}{T_{0r}}$ for binary 0 and $s = -\frac{A}{T_{1f}}$ for binary 1, can be varied according to the required light intensity. By using gradually changing pulses for binary 0 and 1 and an *idle* pulse with constant intensity, it is possible to alleviate both the intra-frame and interframe flicker problems.

Light dimming can be accomplished by changing the slope of the PDSM pulses, i.e., by controlling the T_{0r} and T_{1f} of the binary 0 and 1 pulses, respectively, and by controlling the T_{ir} and T_{if} of the *idle* pulses. The light intensity of a pulse can be reduced by moving T_{0r} to the end of the pulse (for a binary 0 pulse) or by moving T_{1f} to the beginning (binary 1). To provide even more control over the light intensity, the slope can be lowered further below $\frac{A}{T_{0r}}$, as shown in **Fig. 2**. Note that s should not be set so small as to cause the 0 and 1 pulse shapes to become undifferentiable.

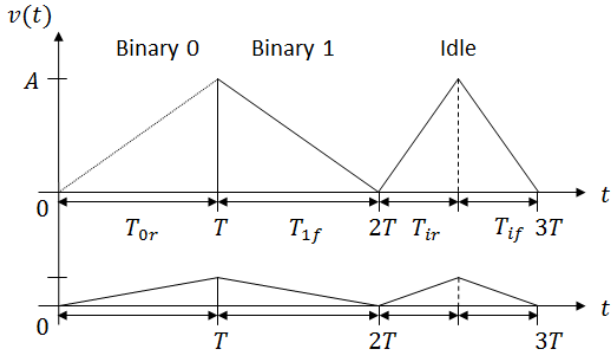

Fig. 2. Pulse dual slope modulation waveform for low-intensity light

The PDSM pulse for binary 0 can be represented mathematically as

$$v_{\mathrm{PDSM}}(t)=\begin{cases} st, & \text{for } 0\le t\le T \\ st, & \text{for } 0\le t\le \frac{A}{s} \\ A, & \text{for } \frac{A}{s}<t\le T \end{cases} \quad \begin{matrix} \text{when } s\le \frac{A}{T} \\ \\ \text{when } s>\frac{A}{T}. \end{matrix} \tag{1}$$

2.2 Spectral Efficiency Comparison

We have chosen VPPM, one of the modulation schemes adopted in IEEE 802.15.7 [6], as a benchmark for comparison with various features of PDSM. The pulse shapes for VPPM are shown in **Fig. 3**, where T_e denotes the VPPM pulse width, which varies according to the light intensity.

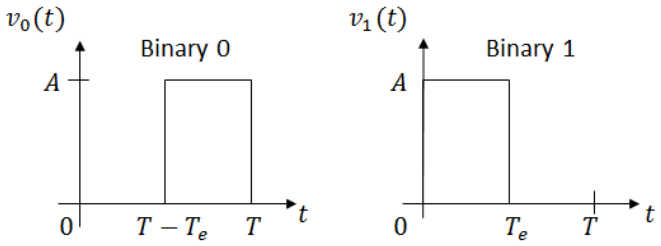

Fig. 3. Pulse shapes for VPPM

The spectral efficiency of pulses used by a modulation scheme is an important factor in conserving spectral resources. To compare the spectral efficiencies of PDSM and VPPM, the spectra of both pulse types can be represented as Fourier transforms. The transform of a PDSM pulse waveform for binary 0, as shown in **Figs. 1** and **2**, is given as follows:

$$V_{\mathrm{PDSM}}(f)=\begin{cases} \frac{s}{(2\pi f)^2}\left(e^{-j2\pi fT}-1\right)-\frac{sT}{j2\pi f}e^{-j2\pi fT}, & \text{if } s\le \frac{A}{T} \\ \frac{s}{(2\pi f)^2}\left(e^{-\frac{j2\pi fA}{s}}-1\right)-\frac{A}{j2\pi f}e^{-j2\pi fT}, & \text{if } s>\frac{A}{T}. \end{cases} \tag{2}$$

The Fourier transform of the VPPM pulse waveform for binary 1 shown in **Fig. 3** is

$$V_{\mathrm{VPPM}}(f) = AT_e e^{-j\pi}\mathrm{sinc}(fT_e), \tag{3}$$

where $\mathrm{sinc}(x) = \frac{\sin(\pi x)}{\pi x}$.

We can define the light intensity index β as $\frac{\text{area of pulse}}{AT}$, where AT is the maximum area of a pulse that is on during the entire symbol duration T of a pulse. Thus, β becomes a relative measure of signal to maximum intensity and has a value $0 < \beta < 1$. **Fig. 4** compares the spectra of PDSM and VPPM pulse waveforms at light intensity indices of 0.25 and 0.75.

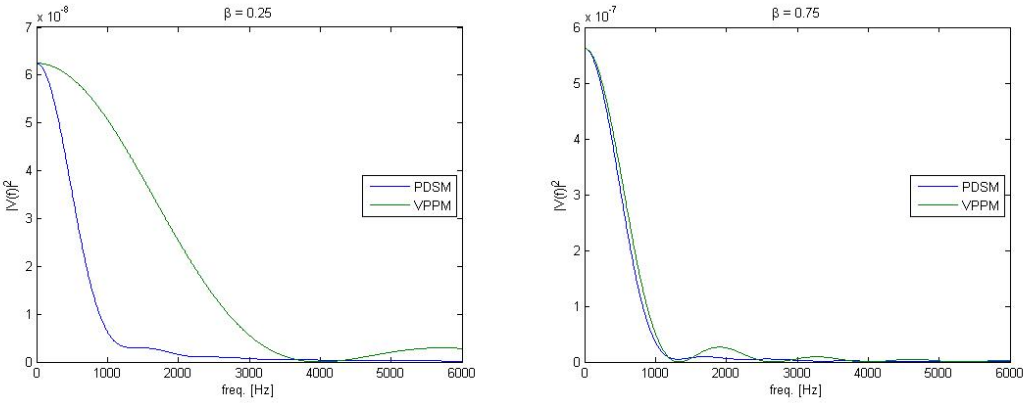

Fig. 4. Power spectra of PDSM and VPPM pulse waveforms

To better illustrate the spectral efficiency of these respective modulation types in terms of the minimum bandwidth needed to form one pulse shape, **Fig. 5** depicts the frequency at which 90% of the total cumulative energy below a specific frequency is covered. For example, when the light intensity index is 0.25, the PDSM pulse covers 90% of the pulse energy below 1334 Hz, whereas the VPPM pulse covers 90% of the pulse energy below 2619 Hz, which means that PDSM uses approximately one half of the required frequency bandwidth required to deliver the VPPM pulse at the same light intensity. **Fig. 5** clearly indicates that the required frequency bandwidth of PDSM stays low over the entire light range.

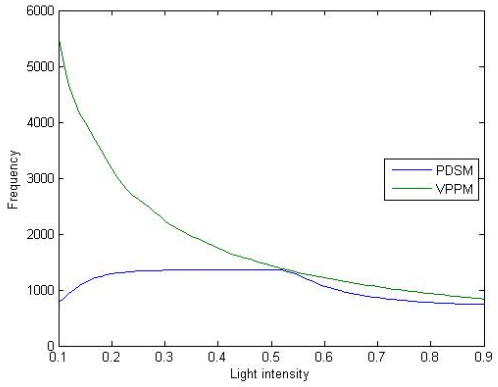

Fig. 5. Frequencies at which the energy level reaches 90%

3. Detection Process

3.1 Dual Sampling Detector

The proposed detection process is very simple and intuitive [14]. At the receiver, a single pulse is sampled twice—during the first and second halves of a symbol duration—and then the two sample values are compared. If the first sample value is higher than the second by more than a marginal value δ, the receiver assumes that a binary 1 was sent, and if the second sample value is higher than the first by more than δ, it assumes that a binary 0 was sent. If the difference between two sampled values is less than δ, the receiver assumes that an *idle* pulse has been sent. **Fig. 6** shows a block diagram of the detection process and the waveforms used.

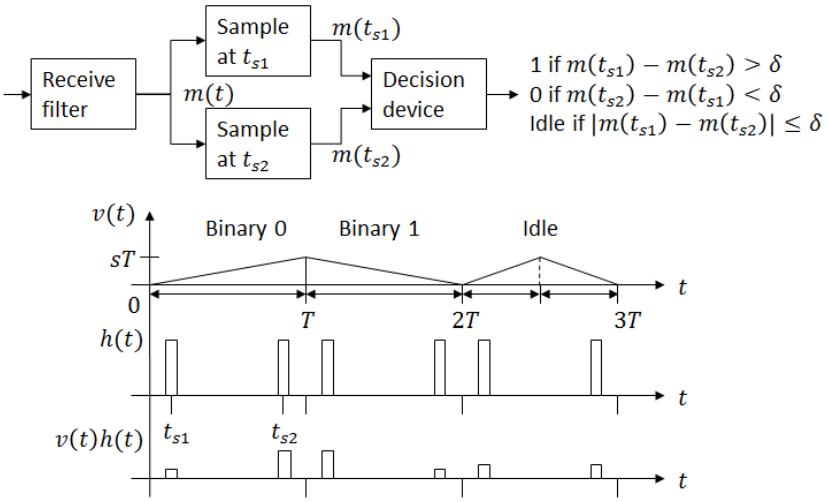

Fig. 6. Dual sampling detection process for PDSM

Within a pulse of duration T, sampling is performed at t_{s1} and t_{s2}, where $t_{s2} = T - t_{s1}$. Owing to the band-limited channel characteristics, and because the low-pass receive filter at the receiver may smooth away an unrealistic abrupt—i.e., vertical—fall or rise at the end of a binary 0 pulse or the beginning end of a binary 1 pulse, respectively, sampling close to the edge may result in incorrect sample values. A low-pass filter (LPF) is used as a receive filter to suppress noise, and to show the effect of an LPF on a PDSM pulse, the LPF outputs of a pulse with light intensity index β = 0.75, $A = 1$, and $T = 1$ ms are drawn in **Fig. 7** for the cutoff frequencies 1, 3, and 10 kHz. It is seen that, when the cutoff frequency is 1 kHz, the second sample value will be significantly rounded, which could result in a detection error. By contrast, the highest cutoff frequency of the LPF (10 kHz) preserves the high-frequency components of the PDSM pulse and therefore allows detection to be performed properly. In this study, the smoothing effect in the received pulse is not considered; that is, we assume that the transmission channel adds only noise and is not band-limited. We also assume that the LPF at the receiver only passes noise components below the cutoff frequency and avoids rounding the pulse edges by always maintaining the cutoff frequency of the LPF at $B = 3$ kHz.

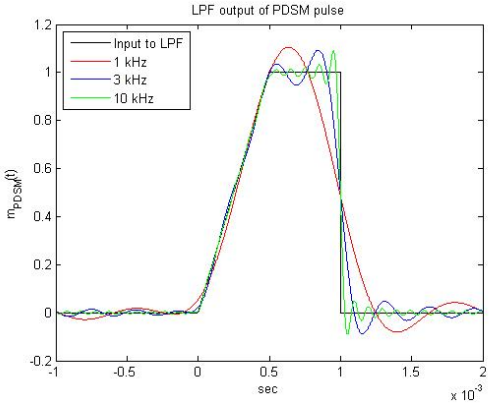

Fig. 7. PDSM pulse output of a low-pass filter

3.2 Error Rates

We will now calculate the bit error rate analytically. The outputs of the samplers at t_{s1} and t_{s2} — $m(t_{s1})$ and $m(t_{s2})$, respectively—in **Fig. 6** are given by

$$\begin{aligned} m(t_{s1}) &= v(t_{s1}) + w(t_{s1}) \\ m(t_{s2}) &= v(t_{s2}) + w(t_{s2}), \end{aligned} \tag{4}$$

where $v(t_s)$ is the sample value at t_s of the transmitted signal and $w(t_s)$ is the sample value of noise at t_s. The signal $v(t_{s2})$ at t_{s2} is given as

$$v(t_{s2}) = \begin{cases} st_{s2}, & \text{if } s \le \frac{A}{t_{s2}} \\ A, & \text{if } s > \frac{A}{t_{s2}}. \end{cases} \tag{5}$$

If the difference between two sample values is x, i.e., $x = m(t_{s2}) - m(t_{s1})$, then x is given by

$$x = \begin{cases} st_{s2} - st_{s1} + w(t_{s2}) - w(t_{s1}), & \text{if } s \le \frac{A}{t_{s2}} \\ A - st_{s1} + w(t_{s2}) - w(t_{s1}), & \text{if } s > \frac{A}{t_{s2}}. \end{cases} \tag{6}$$

This difference can be denoted as a Gaussian random variable X with mean and variance μ_X and σ_X, respectively. In PDSM, the values of $v(t_{s1})$ and $v(t_{s2})$ can be determined from (1) once the light intensity is known.

If it is assumed that the channel noise is an additive white Gaussian noise (AWGN) with power spectral density (PSD) $S_W(f) = \frac{N_0}{2}$ and that the receive filter is an ideal low-pass filter with a cutoff frequency B, then the sample outputs $w(t_{s1})$ and $w(t_{s2})$ owing to noise are random variables that can be denoted as W having identical distributions because the noise can be added to the original pulse at any instant. Thus, the mean of W is zero. Because the autocorrelation $R_W(\tau)$ and the PSD of a random process constitutes a Fourier transform pair, the variance of W is given by

$$\sigma_W^2 = R_W(0) = \int_{-B}^{B} S_W(f)df = \frac{N_0}{2} \cdot 2B = N_0 B. \tag{7}$$

If $w(t_{s1})$ and $w(t_{s2})$ are denoted as W_1 and W_2, respectively, then, because they are independent and identically distributed (*i.i.d.*), the mean and variance of their difference are, respectively

$$\begin{aligned} E[X] &= E[W_2 - W_1] = 2\mu_W = 0 \\ \text{var}[X] &= \text{var}[W_2 - W_1] = 2\sigma_W^2 = 2N_0 B. \end{aligned} \tag{8}$$

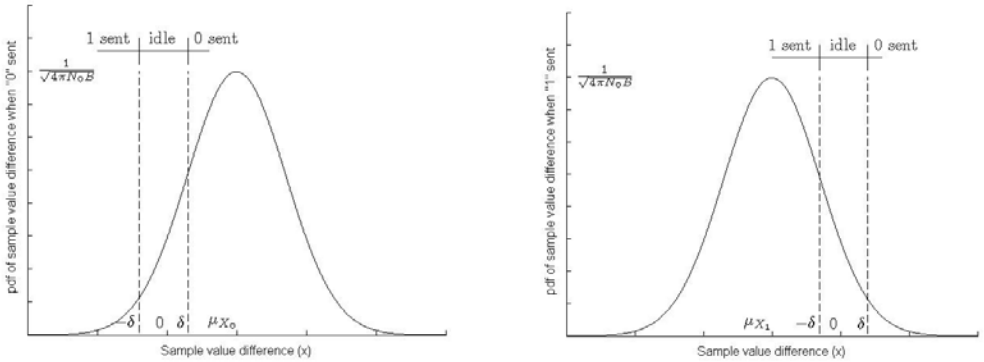

(a) 0 has been sent (b) 1 has been sent

(c) *idle* has been sent

Fig. 8. PDFs of the sample value difference in PDSM

Fig. 8 shows the probability density functions (PDFs) of the difference of the two sample values, with **Figs. 8a**, **b**, and **c** representing cases in which 0, 1, and *idle*, respectively, are sent. In **Fig. 8a**, the area to the left of $x = -\delta$ becomes the probability that channel noise induces the receiver to decide in favor of 1 even though 0 has been sent, whereas the area between $x = -\delta$ and $x = \delta$ indicates the probability that the receiver incorrectly decides in favor of *idle* owing to channel noise. The means of the difference of the sample values for 0, 1, and *idle* $\left(\mu_{X_0}, \mu_{X_1}, \text{and } \mu_{X_i}, \text{respectively}\right)$ are given by

$$\mu_{X_0} = \begin{cases} st_{s2} - st_{s1}, & \text{if s} \le \frac{A}{t_{s2}} \\ A - st_{s1}, & \text{if s} > \frac{A}{t_{s2}} \end{cases} \qquad (9)$$
$$\mu_{X_i} = 0.$$

Note that $\mu_{X_0} = -\mu_{X_1} > 0$ always holds. From (8), the variances of X are identical in all three cases; i.e., $\sigma_{X_0} = \sigma_{X_1} = \sigma_{X_i} = \sqrt{2N_0B}$. Thus, the total bit error probability in the system is

$$p_e = p_0P_{e0} + p_1P_{e1} + p_iP_{ei}, \qquad (10)$$

where $p_0 + p_1 + p_i = 1$. Under the assumption of equiprobable binary 0 and 1, i.e., $p_0 = p_1$, $p_e = p_0(P_{e0} + P_{e1}) + p_iP_{ei}$, the probability of error when 0, 1, and *idle* are sent are given respectively using the Q-function defined as $Q(u) = \frac{1}{\sqrt{2\pi}}\int_u^\infty e^{-\frac{x^2}{2}}dx$ as

$$\begin{aligned} p_{e0} &= P\{X_0 < \delta \mid 0 \text{ sent}\} = \int_{-\infty}^{\delta} f_{X_0}(x|0)dx = \int_{-\infty}^{\delta} \frac{1}{\sqrt{2\pi\sigma_{X_0}}} e^{-\frac{(x-\mu_{X_0})^2}{2\sigma_{X_0}^2}} dx \\ &= Q\left(\frac{\mu_{X_0}-\delta}{\sigma_{X_0}}\right) \\ p_{e1} &= P\{X_1 > -\delta \mid 0 \text{ sent}\} = \int_{-\infty}^{\delta} f_{X_1}(x|1)dx = \int_{-\delta}^{\infty} \frac{1}{\sqrt{2\pi\sigma_{X_1}}} e^{-\frac{(x-\mu_{X_1})^2}{2\sigma_{X_1}^2}} dx \\ &= Q\left(-\frac{\delta+\mu_{X_1}}{\sigma_{X_1}}\right) = Q\left(\frac{|\mu_{X_1}|-\delta}{\sigma_{X_1}}\right) = P_{e0} \\ p_{ei} &= P\{|X_i| > \delta \mid idle \text{ sent}\} = 1 - \int_{-\delta}^{\delta} f_{X_i}(x|idle)dx = 2\int_{\delta}^{\infty} \frac{1}{\sqrt{2\pi\sigma_{X_i}}} e^{-\frac{(x-\mu_{X_i})^2}{2\sigma_{X_i}^2}} dx \\ &= 2Q\left(\frac{\delta-\mu_{X_i}}{\sigma_{X_i}}\right) = 2Q\left(\frac{\delta}{\sigma_{X_i}}\right). \end{aligned} \qquad (11)$$

The total bit error probability then becomes

$$\begin{aligned} p_e &= p_0(P_{e0} + P_{e1}) + p_iP_{ei} = 2p_0P_{e0} + p_iP_{ei} \\ &= 2p_0Q\left(\frac{\mu_{X_0}-\delta}{\sigma_{X_0}}\right) + 2p_iQ\left(\frac{\delta}{\sigma_{X_i}}\right). \end{aligned} \qquad (12)$$

Fig. 9 shows graphs of both the simulated and analytical BERs of a PDSM signal with $A = 1$, $T = 1$ ms, $p_i = 0.1$, $\delta = 0.1$ V, $N_0 = 10^{-6}$ J, and $B = 3 \times 10^3$ Hz.

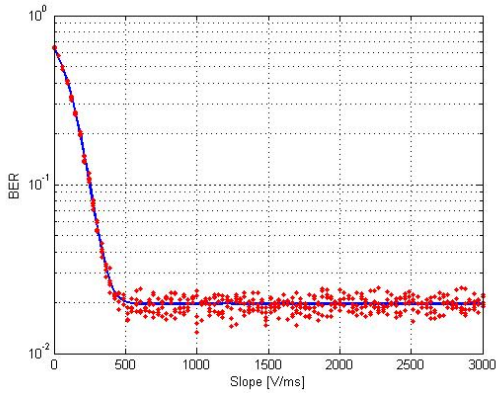

Fig. 9. BERs of PDSM detection from analysis and simulation

Note that the light intensity β can easily be substituted for the slope of the *x*-axis in **Fig. 9** using the following slope and light intensity relationship:

$$s = \begin{cases} 2\beta A, & \text{if } s \le \frac{A}{T} \\ \frac{A}{2(1-\beta)T}, & \text{if } s > \frac{A}{T} \end{cases} \tag{13}$$

Fig. 10 shows the BER versus slope for various sets of measurement parameters for a pulse with amplitude $A = 1$ and width $T = 1$ ms.

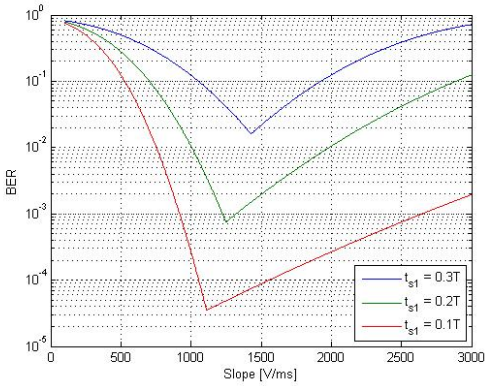

(a) $\frac{t_{s1}}{T} = 0.1, 0.2, 0.3$, $p_i = 0$, $N_0 = 5 \times 10^{-6}$ W/Hz, $B = 3 \times 10^3$ Hz, $\delta = 0.2$

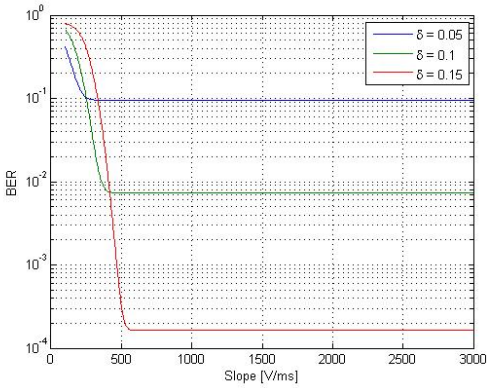

(b) $\delta = 0.05, 0.1, 0.15$, $\frac{t_{s1}}{T} = 0.2$, $p_i = 0.2$, $N_0 = 3 \times 10^{-7}$ W/Hz, $B = 3 \times 10^3$ Hz

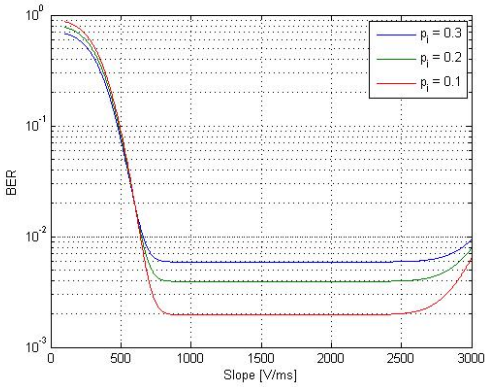

(c) $p_i = 0,1, 0.2, 0.3$, $\delta = 0.2$, $\frac{t_{s1}}{T} = 0.2$, $N_0 = 1 \times 10^{-6}$ W/Hz, $B = 3 \times 10^3$ Hz

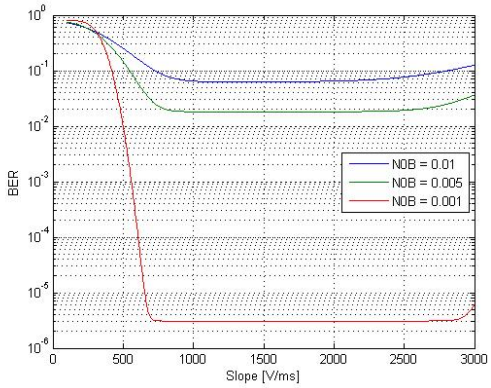

(d) $N_0B = 0.01, 0.005, 0.001$, $p_i = 0.2$, $\delta = 0.2$, $\frac{t_{s1}}{T} = 0.2$

Fig. 10. BER vs. slope for various measurement parameters

Fig. 10a shows the BER for $p_i = 0$ as the second sampling instant $\frac{t_{s1}}{T}$ is varied from 0.1 to 0.3 (or equivalently, as $\frac{t_{s2}}{T}$ is varied from 0.9 to 0.7). The lowest BER for a fixed sampling instant is always obtained when the second sampling is performed at the point where the hypotenuse and flat section of the binary 0 pulse meet. When the slope s is small, the BER increases because the corresponding low light condition reduces the difference between two given sample values; as the light intensity increases, the second sample value in the binary 0 case remains the same ($v(t_{s2}) = A$), but the first sample value increases, which reduces the difference between the two sample values. The figure also shows that lower BERs are obtained when the distance between two sampling instants increases, as this increases the sample value difference. **Fig. 10b** shows the change in the BER as the decision range δ in favor of *idle* varies, from which it can be seen that increasing δ reduces the BER. This is a result of the fact that, as δ increases in (12), $P_{ei} = 2Q\left(\frac{\delta-0}{\sigma_{X_i}}\right)$ decreases much faster than $P_{e0} = Q\left(\frac{\mu_{X_0}-\delta}{\sigma_{X_0}}\right)$ (or equivalently, P_{e1}) increases, which in turn reduces the BER. Note that changes in u affect $Q(u)$ to a greater degree when u is small, as can be easily deduced from the shape of the Gaussian PDF. This means that the distance between 0 and δ in $P_{ei} = 2Q\left(\frac{\delta-0}{\sigma_{X_i}}\right)$ is large relative to the distance between δ and μ_{X_0} in $P_{e0} = Q\left(\frac{\mu_{X_0}-\delta}{\sigma_{X_0}}\right)$, and thus $P_{e0} \ll P_{ei}$. **Fig. 10c** shows the change in the BER as the probability of *idle* (p_i) varies, from which it is seen that lower values of p_i correspond to a slightly lower BER. Although varying p_i changes neither P_{e0} nor P_{ei} as in (12), $P_{e0} \ll P_{ei}$—as is the case in **Fig. 10b**—and therefore p_i plays a greater role than p_0 in determining the BER. **Fig. 10d** shows the change in the BER as the noise PSD and the cutoff bandwidth product N_0B varies. Note that N_0B affects only σ_X in (12); when N_0B increases tenfold, σ_X increases $\sqrt{10} = 3.162$ times in (8), which reduces both P_{e0} and P_{ei} by a significant amount, as shown in **Fig. 10d**.

3.2 Comparison using the Correlation Detector

To develop a correlation detector for PDSM and VPPM, we start with a case in which there is no *idle* pulse, i.e., the source sends only binary 0 or 1, before expanding this analysis to investigate a case including binary 0, 1, and *idle*.

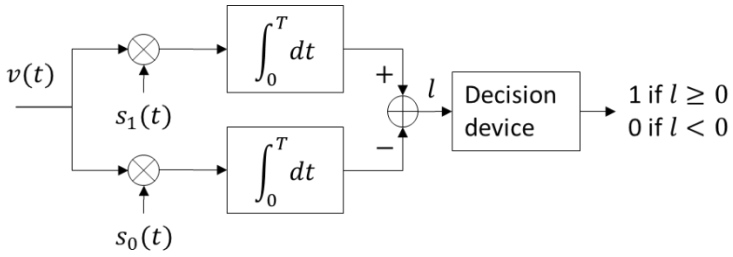

Fig. 11. Correlation detector for PDSM and VPPM without *idle*

Fig. 11 shows a correlation detector that can be used to detect binary 0 and 1. It is well known that the BER of a correlation receiver is $P_e = Q\left(\sqrt{\frac{E_b(1-\rho)}{N_0}}\right)$, where $E_b = \frac{1}{E_b}\int_0^T s_0^2(t)dt$ and $\rho = \frac{1}{E_b}\int_0^T s_0(t)s_1(t)dt$ [15]. Then, for a VPPM signal,

$$\rho = \begin{cases} 0, & \beta < 0.5 \\ \frac{2\beta-1}{\beta}, & \beta \geq 0.5, \end{cases} \tag{14}$$

and the BER of the VPPM signal can be calculated using the correlation detection relation above as

$$P_e = \begin{cases} Q\left(A\sqrt{\frac{\beta T}{N_0}}\right), & \beta < 0.5 \\ Q\left(A\sqrt{\frac{\beta T(1-\rho)}{N_0}}\right), & \beta \geq 0.5, \end{cases} \tag{15}$$

where β is the light intensity index. For a PDSM signal,

$$\rho = \begin{cases} 0.5, & 0 < \beta < 0.5 \\ \frac{3-12\beta+24\beta^2-16\beta^3}{8(1-\beta)^2(4\beta-1)}, & 0.5 \leq \beta < 0.75 \\ \frac{3(2\beta-1)}{4\beta-1}, & 0.75 \leq \beta < 1, \end{cases} \tag{16}$$

and, using the correlation detection relation, the BER of the PDSM signal becomes

$$P_e = \begin{cases} Q\left(2\beta A\sqrt{\frac{T(1-\rho)}{3N_0}}\right), & \beta < 0.5 \\ Q\left(A\sqrt{\frac{T(4\beta-1)(1-\rho)}{3N_0}}\right), & \beta \geq 0.5. \end{cases} \tag{17}$$

To determine the BER of a PDSM signal using dual sampling, (12), with $p_i = 0$, is used in conjunction with (13). Three BER graphs of PDSM and VPPM at various values of β are shown in **Fig. 12**. Here, $A = 1$, $T = 1$ ms, $\frac{t_{s1}}{T} = 0.2$, $N_0 = 10^{-5}$ W/Hz, and $B = 3 \times 10^3$ Hz, with $\frac{t_{s1}}{T}$ and B used only for the case where PDSM is detected using dual sampling. It is seen that the rectangular VPPM pulse provides a significantly better BER performance than do the slanted PDSM pulses over the entire light intensity range. For the PDSM signals, the correlation detection method performs better than the dual sampling detection method over the entire light intensity range as well as when no *idle* pulse transmission occurs; these results confirm the advantage of using a matched filter for various pulse shapes.

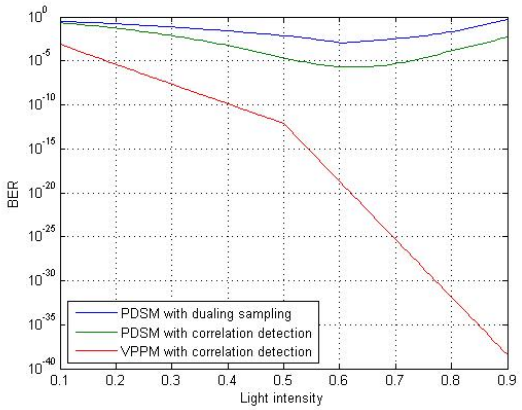

Fig. 12. BER vs. light intensity when $p_i = 0$

We next consider the case in which *idle* transmission occurs, i.e., $p_i > 0$. To model a VPPM signal with *idle* pulses, we create an *idle* pulse located in the center of a pulse with a duration corresponding to a constant area for binary 0 or 1, as shown in **Fig. 13**.

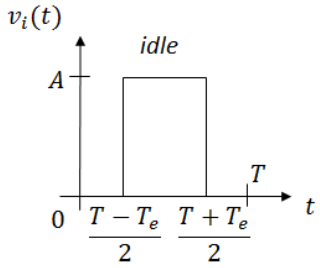

Fig. 13. *Idle* pulse shape for VPPM

When there is an *idle* transmission, the correlation detector is implemented as shown in **Fig. 14**. At the decision stage, the receiver chooses the symbol that yields the highest integrator output.

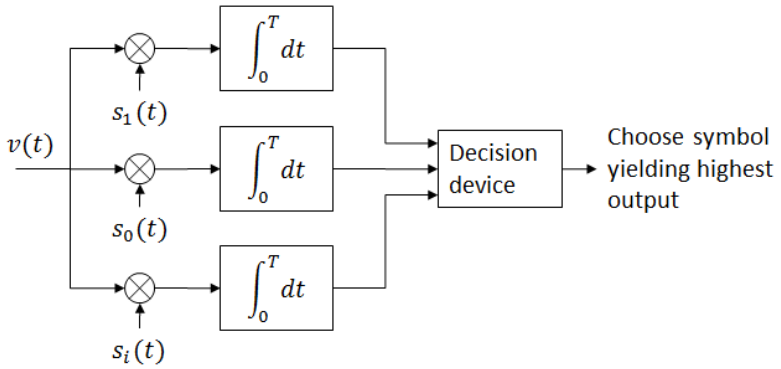

Fig. 14. Correlation detector for PDSM and VPPM with an *idle* probability

Because two given correlator output differences will not be independent when three pulse shapes overlap, it is not easy to formulate the BER mathematically in closed form when $p_i > 0$; therefore, we used a Monte Carlo simulation to determine the BER of correlation detection for PDSM and VPPM signals that include the *idle* state, and we used (12) to determine the BER of PDSM using dual sampling. The results are given in **Fig. 15** for signals with $A = 1$, $T = 1$ ms, $N_0 = 5 \times 10^{-5}$ W/Hz, $\frac{t_{s1}}{T} = 0.2$, $B = 3 \times 10^3$ Hz, and $\delta = 0.1$ V, where $\frac{t_{s1}}{T}$, B, and δ are used only for PDSM dual sampling detection. For the simulation, 10^5 bits were transmitted. The figure shows that the BER of PDSM using dual sampling detection is lower than that of PDSM using correlation detection over the entire light intensity range when $p_i < 0.08$, whereas for $p_i > 0.08$, the BER produced by dual sampling becomes increasingly higher at low light intensities. The figure also shows that the BER of VPPM changes sharply in value at $\beta = \frac{1}{3}$ because the light intensities of the binary 0, 1, and *idle* rectangular pulses at this intensity index evenly cover the bit duration without overlapping, representing the point at which the three correlators produce maximum mutual differences and thus produce the lowest BER. However, as β changes to either a higher or lower light intensity index than $\frac{1}{3}$, the values produced by the correlators begin to converge, which results in smaller differences and, in turn, a higher BER.

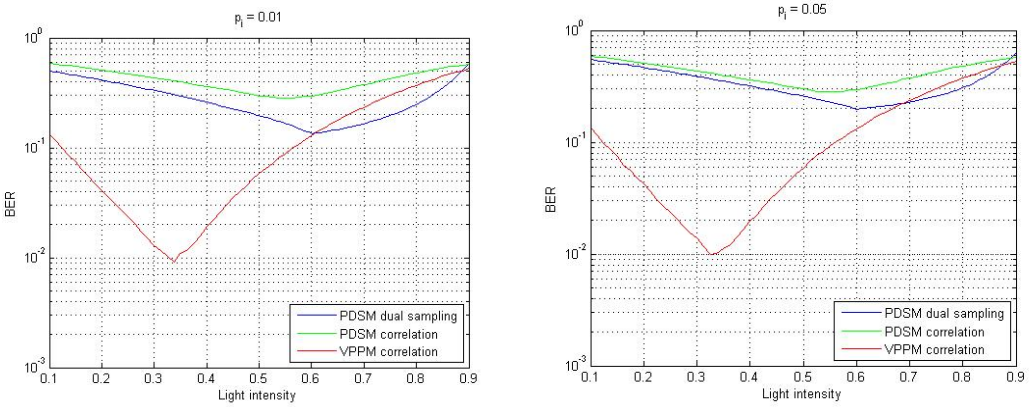

(a) $p_i = 0.01$ (b) $p_i = 0.05$

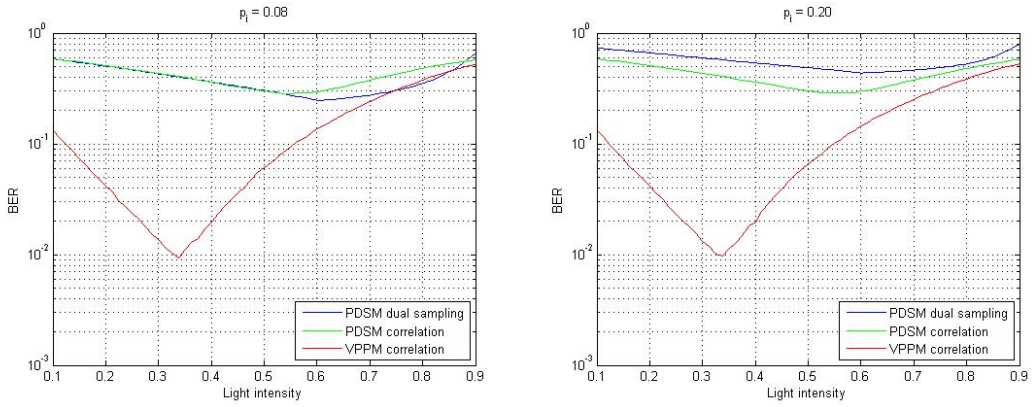

(c) $p_i = 0.08$ (d) $p_i = 0.2$

Fig. 15. BERs of PDSM for $\frac{t_{s1}}{T} = 0.2$, $N_0 = 5 \times 10^{-5}$ W/Hz, $B = 3 \times 10^3$ Hz, and $\delta = 0.1$

4. Conclusion

This paper introduced the use of pulse dual slope modulation (PDSM) as a way of improving spectral efficiency. A simple and intuitive PDSM detection method was then produced. We performed a comprehensive investigation that revealed the beneficial features of PDSM, and its pulse shape was proven to be spectrally more efficient than that of a variable pulse position modulation (VPPM) pulse over the entire light intensity range. We also proposed using a symmetrical dual slope pulse to denote the *idle* period to avoid intra-frame flicker. We derived a mathematical description for the bit error rate (BER) of PDSM signal detection using the proposed scheme and validated it through simulation. For comparison, we applied a correlation detection method to PDSM and VPPM signals, showing that, for $p_i < 0.08$, the BERs of PDSM signals detected using dual sampling were lower than those of PDSM signals obtained using correction detection over the entire light intensity range, and both performed worse than VPPM using correlation detection. For $p_i > 0.08$, however, PDSM using correlation began to perform better at low light intensities. Overall, our investigation showed that detection of PDSM signals using dual sampling features constitutes a simple, well performing detection method in terms of reducing spectral usage and flicker and improving BER performance, even though this is achieved within a specific light intensity range and with a limited *idle* transmission probability.

Acknowledgement

This work was supported by the “GRRC” Project of the Gyeonggi Provincial Government.

References

[1] O. Bouchet, M. Wolf, M. E. Tabach, T. Kamalakis, F. Grahame, J. Walewski, S. Nerreter, M. Franke, J. Grubor, D. O’Brien, and K. D. Langer, “Hybrid wireless optics (HWO): Building the next-generation home network,” In *Proc. of The 6th Int. Symp. On Communications Systems, Networks, and Digital Processing*, pp. 283-287, 2008. Article (CrossRef Link)

[2] F. R. Gfeller and U. Bapst, “Wireless in-house data communication via diffuse infrared radiation,” *IEEE*, vol. 67, pp. 1474-1486, November, 1979. Article (CrossRef Link)

[3] D. O’Brien, L. Zeng, Hoa Le-Minh, G. Faulkener, J. W. Walewski, and S. Randel, “Visible light

communications: Challenges and possibilities," In *Proc. of IEEE 19th Int. Symp. on Personal, Indoor and Mobile Radio Communications*, pp. 1-5, 2008. Article (CrossRef Link)
[4] Y. Tanaka, S. Haruyama, and M. Nakagawa, "Wireless optical transmissions with white colored LED for wireless home links," In *Proc. of IEEE 19th Int. Symp. on Personal, Indoor and Mobile Radio Communications*, pp. 1325-1329, 2000. Article (CrossRef Link)
[5] S. Rajagopal, R. D. Roberts, and S. Lim, "IEEE 802.15.7 Visible light communication: modulation schemes and dimming support," *Communication Magazine*, vol. 50, pp. 72-82, March, 2012. Article (CrossRef Link)
[6] S. M. Berman, D. S. Greenhouse, I. L. Bailey, R. Clear, and T. W. Raasch, "Human electroretinogram responses to video displays, fluorescent lighting and other high frequency sources," *Optometry and Vision Science*, vol. 68, pp. 645-662, 1991. Article (CrossRef Link)
[7] *IEEE Standard for Local and Metropolitan Area Networks, Part 15.7: Short-Range Wireless Optical Communication Using Visible Light*, IEEE Std. 802.15.7, 2011. Article (CrossRef Link)
[8] Y. Zhang, Z. Zhang, Z. Huang, H. Cai, L. Xia, and J. Zhao, "Apparent brightness of LEDs under different dimming methods," *SPIE*, vol. 6841, p. 684109, 2007. Article (CrossRef Link)
[9] S. Muthu, F. J. Schuurmans, and M. D. Pashley, "Red, green, and blue LED based white light generation: Issues and control," In *Proc. of The 37th Annu. IEEE-IAS Meeting*, vol. 2, pp. 327-333, 2002. Article (CrossRef Link)
[10] X. Ma, K. Lee, and K. Lee, "Appropriate modulation scheme for visible light communication systems considering illumination," *Electronics Letters*, vol. 48, pp. 1137-1139, 2012. Article (CrossRef Link)
[11] R. D. Roberts, S. Rajagopal, and S. Lim, "IEEE 802.15.7 physical layer summary," In *Proc. of GLOBECOM Workshops*, pp. 772-776, 2011. Article (CrossRef Link)
[12] J. Das, "Pulse slope modulation – A new method of modulating video pulses and its possible applications on the line circuits," *Indian J. Physics*, vol. 28, pp. 449-462, 1954.
[13] M. Anand and P. Mishra, "A novel modulation scheme for visible light communication," In *Proc. of 2010 Annual IEEE India Conference (INDICON)*, pp. 1-3, 2010. Article (CrossRef Link)
[14] M. Oh, "A flicker mitigation modulation scheme for visible light communications," In *Proc. of International Conference on Advanced Communication Technology (ICACT)*, pp. 933-936, 2013. Article (CrossRef Link)
[15] S. Haykin and M. Moher, *Communication Systems 5/e*, John Wiley & Sons, 2010. Article (CrossRef Link)

Minseok Oh is an associate professor in the Department of Electronic Engineering, Kyonggi University, Suwon, Korea. He received the B.S. degree from Seoul National University, Seoul, Korea in 1987, the M.S. degree from Columbia University, New York, U.S.A. in 1993, and the D.Sc. degree from Washington University, St. Louis, U.S.A., in 1998; all of these degrees were in electrical engineering. His current interests include wireless mesh networks and visible light communications. Before joining academia, Dr. Oh worked as a senior research engineer for LG Telecom, Korea, from 2000 to 2003 and as a technical consultant for AT&T, NJ in 1999.